J Clust Sci (2017) 28:1825–1836
DOI 10.1007/s10876-017-1186-0

ORIGINAL PAPER

# Effect of P-Containing Ligands on the Structural and Optical Properties of $(CdSe)_n$ (n = 3, 6, 10) Clusters

**Sheng-Ping Yu[1,2] · De-Lin Huang[2] · Zhi-Gang Zhao[2] · Ming-Li Yang[1] · Ming-Hui Yang[3]**

Received: 4 May 2016 / Published online: 3 March 2017


**Abstract** The effect of phosphorus-containing ligands on the structure, energetics and properties of the $(CdSe)_n$ clusters (n = 3, 6, and 10) with different number of $PH_3$ and $PMe_3$ ligands were studied by using density functional theory calculations. The P atom in the ligand interacts with Cd and forms a strong Cd–P coordination bond. The introduction of ligands does not change the cluster architecture, but leads to considerable changes in Cd–Se bondlength, charge distribution, binding energy, HOMO–LUMO gap and optical absorption. The ligand influence is enhanced with increasing ligand coverage. A blueshift in absorption band was predicted for the clusters with increasing ligands, resulting from the electron donating characteristics of the ligands that hamper electron transition from Se to Cd. As P-containing ligands are often used in the preparation of CdSe nanocrystals, our calculations reveal the influence of ligand-cluster interaction on the cluster geometrical and electronic properties, which would be helpful for the nanocrystal design and synthesis.

**Electronic supplementary material** The online version of this article (doi:10.1007/s10876-017-1186-0) contains supplementary material, which is available to authorized users.

✉ Sheng-Ping Yu
ysp1998@163.com

✉ Zhi-Gang Zhao
zzg63129@163.com

[1] Institute of Atomic and Molecular Physics, Sichuan University, Chengdu, 610065, China

[2] College of Chemistry and Environment Protection Engineering, Southwest University for Nationalities, Chengdu 610041, China

[3] State Key Laboratory of Magnetic Resonance and Atomic and Molecular Physics, Wuhan Institute of Physics and Mathematics, Chinese Academy of Sciences, Wuhan 430071, China

**Keywords** Ligand effect · CdSe clusters · Optical properties · First-principles calculations

## Introduction

II–VI semiconductor nanocrystals (NCs) have seen wide applications in solar cells, light emitting diodes and biological images [1]. The NCs exhibit interesting properties that vary with their sizes, shapes and capping ligands [2–7]. Among various NCs, colloidal NCs attract special attention because of their high yield, high quality and low cost in preparation. The colloidal NCs are usually composed of a semiconductor core coated by organic ligands which are well recognized as a key factor in synthesis, manipulation and application [8]. In addition, the surface ligands, such as phosphine, phosphine oxide and amines, play an important role in stabilizing the NCs and have strong effect on the electronic and optical properties of the passivated NCs. Explorations on the ligand-NCs interaction are helpful for the design and preparation of high-quality NCs.

While computational studies have shown many advantages in exploring the structures and properties of atoms, molecules and solids, the prepared NCs are usually 1–100 nm in diameter, a size difficult for computational studies at first-principles level. Computations on small-sized II–VI clusters are an alternative but effective way to provide useful information on the structural and electronic properties of these NCs. In fact, many studies have been conducted to the small II–VI clusters, in particular to the CdSe clusters, over the past decades [9–30].

The structures of pure $(CdSe)_n$ clusters have been studied at density functional theory (DFT) level for n = 1–16 [10–15], 17 [16], 33 [13–17], 45 [13], 6–54 [14] and 111 [15]. Planar and cyclic structures were predicted for $n \leq 6$ and three dimensional structures for larger sizes. The surface ligands, such as $NH_3$ [18, 19], trioctylphosphine [20], trimethyl phosphine oxide (TMPO) [19, 21, 22], cysteine [23, 24], thiolate (SR) and SR-COOH [25–27], bis (diselenophosphinate) [28] and amines [19, 29, 30], lead to significant changes in the structures, energetics and optical properties of CdSe clusters. For example, Yang et al. [19]. have studied computationally the effect of different ligands on the structures and energetics of $(CdSe)_2$. The binding energies for various ligands decrease in the order of $OPMe_3 > OPH_3 > NH_2Me > NH_3 > NMe_3 > PMe_3 > PH_3$ for neutral clusters at the B3LYP/Lanl2DZ level. Albert et al. [21]. have assessed the performance of various exchange–correlation functionals in predicting the binding energy (BE) in $Cd_{33}Se_{33}$-TMPO and found that the BE values are insensitive to the functionals. Chung et al. [23]. performed DFT and time-dependent DFT (TDDFT) calculations on the structures and optical absorption of electronic excitation energies of cysteine-capped $(CdSe)_n$ of n = 3, 6, 10 and 13. In our previous studies [24, 28], the ligand-$(CdSe)_n$ interaction and its influence on the optical absorptions of cadmium bis(diselenophosphinate) and cysteine-capped $(CdSe)_n$ clusters of n = 1–10, 13, 16 and 19 have been studied using DFT and TDDFT calculations. The functional and basis set dependence, solvent effect, and adsorption pattern of the ligands were systematically addressed for these ligated CdSe clusters. It was found that the

ligands adsorb chemically onto the clusters and lead to remarkable changes in their optical absorption spectra.

Although many studies [18–30] have been devoted to the studies of ligated CdSe clusters, the ligand effect on their structures and properties is still far from clear. Part of the difficulty comes from the complexity in the preparation of CdSe clusters during which various chemical components may coexist and affect the cluster nucleation and growth. Using ligands with various reactivities and selectivities to control the reactions has become a common approach to obtain clusters with specific sizes, shapes, and structures. The phosphorus-containing ligands have been widely used in the preparation of II–VI NCs [18–22]. However, their interaction with the II–VI cluster cores has not yet been well addressed. In this work, we performed a first-principles study on the $(CdSe)_n$ ($n = 3$, 6, and 10) clusters capped with P-containing ligands. Experimentally, the P-containing ligands usually have one or more long aliphatic chains or benzene derivatives. In our calculations, a simplified ligand model of using $PH_3$ and $PMe_3$ to replace aliphatic or cyclic hydrocarbons was used to mimic the ligand effect. This is a reasonable simplification since the carbon atoms in the ligands do not adsorb directly onto the CdSe clusters. Instead, they affect the cluster via the P atom in the ligand. The carbon atom farther than the carbon atom bonding with the P atom should have limited effect on the clusters. Using this simplified model, we studied the structure and electronic properties of CdSe clusters of $n = 3$, 6 and 10 when the cluster is gradually capped by $PH_3$ and $PMe_3$.

## Computational Methods

The initial structures of $(CdSe)_3$, $(CdSe)_6$ and $(CdSe)_{10}$ were taken from previous studies [18, 23–25] and reoptimized, with the Tao-Perdew-Staroverov-Scuseria (TPSS) [31] functional and Weigend's def2-TZVP [32] basis set, as implemented in the Turbomole program [33]. To locate the most favorable adsorbing patterns of $PH_3$ on the $(CdSe)_n$ surfaces, we constructed various candidate structures for the adsorbed $(PH_3)_m$-$(CdSe)_n$ systems and then optimized at the same level. Both the singlet and triplet states were examined for all the species. As shown in Table S1, the singlet states were found more stable than their corresponding triplet states for all the structures. Therefore, only the calculations for the singlet-state structures were discussed. The Cartesian coordinates of all the presented structures were given in Table S2 in the supplementary materials. On the basis of our calculations of CdSe-$PH_3$ structures, we carried out calculations for CdSe-$PMe_3$ structures by replacing $PH_3$ with $PMe_3$. In order to verify the obtained structures are true minima on the potential energy surface, the structures are computed using harmonic vibrational frequency calculations. The frequencies of the most stable structures were given in Table S3. For comparison, the structures were also optimized using Perdew-Burke-Ernzerhof (PBE) [34] and Becke-Lee–Yang–Parr (BLYP) functionals [35, 36]. As shown below, the same energy orders were produced with the three functionals. For the Cd atoms, the effective core potential with relativistic correction of Wood-Boring [37] was used to describe the core electrons, whereas the

valence electrons 4*s*, 4*p*, 4*d* and 5*s* were described with triple split-valence basis set plus an augmented polarization function. The resolution-of-the-identity (RI) approximation [38] and multipole accelerated RI (MARI) approach [39] were applied to speed up the calculations. To validate our computational strategy, we computed Cd–Se bond length of $(CdSe)_3$, which is 2.50 Å and agrees well with that reported by Maroulis et al. (2.54 Å) [11]. TDDFT calculations [40] were performed to predict the optical absorption spectra of the structures with PBE functional. In the TDDFT calculations, the self-consistent-field convergence criteria were tightened to $10^{-7}$ au in density. To produce the absorbing bands of interest, the lowest one hundred excitations were calculated. Further analysis was carried out using Natural Bond Orbital NBO6.0 program [41] at the PBE0 [34] /Lanl2DZ [42, 43] level with the Gaussian 09 package [44].

## Results and Discussion

### Bare $(CdSe)_n$ Clusters

The most-stable structures of bare $(CdSe)_n$ (n = 3, 6 and 10) clusters are basically the same with other studies [9, 18, 23–25], as shown in Fig. 1 $(CdSe)_3$ possesses a ring structure with $D_{3h}$ symmetry. $(CdSe)_6$ has $D_{3d}$ symmetry and can be considered as an antiparallel stacking of two $(CdSe)_3$. $(CdSe)_{10}$ consists of two $(CdSe)_6$ with a shared $(CdSe)_2$. These three clusters are characterized by their hexagonal $(CdSe)_3$ rings, which are the building blocks of CdSe clusters. Previous studies [23, 24] have revealed that the clusters with n = 3, 6 and 10 are more stable than their neighbors. In all these structures, the Cd and Se atoms stand alternatively. The averaged coordination numbers of Cd and Se are the same in a cluster, but change with cluster size, 2 in $(CdSe)_3$, 3 in $(CdSe)_6$ and 3.2 in $(CdSe)_{10}$. Table 1 lists their averaged Cd-Se bond lengths, which increase by 0.169 Å from n = 3 to 6, but are shortened slightly (0.017 Å) from n = 6 to 10.

### Ligand Capped $(CdSe)_n$ Clusters

The lowest-energy structures of CdSe-$PMe_3$ are presented in Fig. 1, while those of $PH_3$-capped $(CdSe)_n$ clusters are given in Supplementary material (Figures S1, S2 and S3). The three functionals, TPSS, BLYP and PBE, produce the same energy orders for the isomers, as shown in Tables S4 and S5. The CdSe-$PMe_3$ cluster structures are similar to those with $PH_3$ attachment. The P atom of the ligands always interacts with the Cd atom in the cluster, while the bonding between P and Se is unstable. Yang et al. [18, 19] also found that the P in a P-containing ligand tends to bond with Cd. The cluster structures have some changes when the ligands attach to the clusters one by one, but the three clusters of n = 3, 6, 10 basically retain their architectures after ligand attachment.

The averaged Se–Cd and P–Cd bondlengths of the CdSe-$PMe_3$ clusters are listed in Table 1. For n = 3, the averaged Se−Cd bond length is longer than that in bare cluster by 0.008 Å, and increases slightly with ligand number, and so do the P−Cd

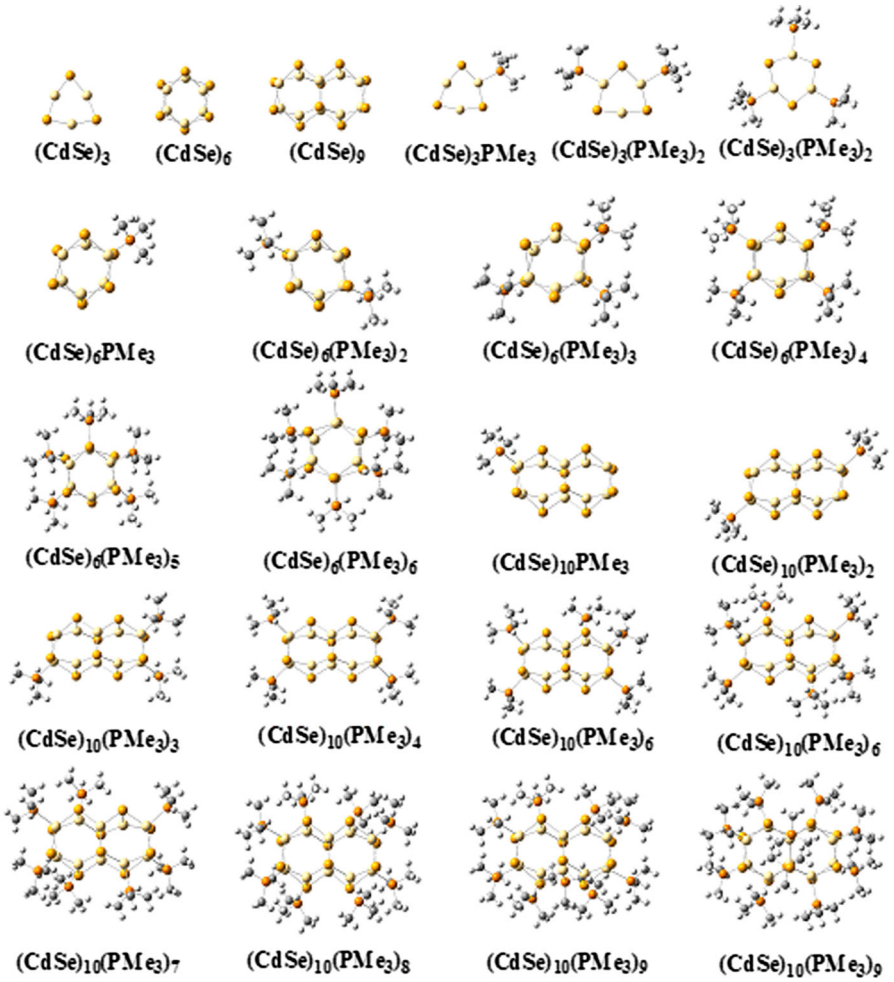


**Fig. 1** Structures of bare $(CdSe)_n$ and the most stable $(CdSe)_n(PMe_3)_m$(n = 3, 6, 10; m = 1–n) optimized at TPSS/def2-TZVP level. Cd = *yellow*, Se = *gold*, C = *grey*, P = *orange*, and H = *silver* (Color figure online)

bonds. For n = 6 and 10, similar variations were noted for the Se−Cd and P–Cd bonds. In the ligated clusters, Cd atoms bond with the ligands while they bond with Se. Affected by the P–Cd bonding, the Cd–Se bonds are therefore weakened and elongated. There are several possible interacting sites when two or more ligands interact with the cluster. For example, the two ligands have three combinations when interact with $(CdSe)_6$. From the most stable structures show in Fig. 1, the combinations in which the ligands have the farthest distances are more stable than other combinations. The steric hindrance of ligands becomes significant when the number of ligands increases. The averaged P−Cd bond lengths decrease with clusters size when the clusters possess the same number of ligands. For the clusters

**Table 1** Average Se–Cd bond length (in Å), Average P–Cd bond length (in Å), Net charge (in au), Binding energy (*BE*, in eV), Enthalpy (ΔH, in eV, T = 298 K), Gibbs free energy (ΔG, in eV, T = 298 K) and HOMO–LUMO gaps (Δε, in eV) of $(CdSe)_n(PMe_3)_m$(n = 3, 6 and 10; m = 1−n) complexes

| | Average Bond Length | | Net Charge $(PMe_3)_m$ | *BE* | ΔH | ΔG | Δε |
|---|---|---|---|---|---|---|---|
| | Se–Cd | P–Cd | | | | | |
| $(CdSe)_3$ | 2.497 | – | – | – | – | | 2.692 |
| $(CdSe)_3PMe_3$ | 2.505 | 2.698 | 0.22 | 0.74 | −0.27 | −0.67 | 2.986 |
| $(CdSe)_3(PMe_3)_2$ | 2.514 | 2.731 | 0.40 | 0.64 | −0.38 | −1.16 | 3.163 |
| $(CdSe)_3(PMe_3)_3$ | 2.523 | 2.777 | 0.53 | 0.56 | −0.32 | −1.48 | 3.273 |
| $(CdSe)_6$ | 2.666 | – | – | – | – | | 2.348 |
| $(CdSe)_6PMe_3$ | 2.669 | 2.650 | 0.24 | 0.85 | −0.32 | −0.81 | 2.503 |
| $(CdSe)_6(PMe_3)_2$ | 2.670 | 2.648 | 0.46 | 0.82 | −0.68 | −1.54 | 2.709 |
| $(CdSe)_6(PMe_3)_3$ | 2.678 | 2.663 | 0.65 | 0.76 | −0.88 | −2.08 | 2.822 |
| $(CdSe)_6(PMe_3)_4$ | 2.683 | 2.673 | 0.84 | 0.72 | −0.96 | −2.62 | 2.935 |
| $(CdSe)_6(PMe_3)_5$ | 2.688 | 2.694 | 0.99 | 0.66 | −1.04 | −3.01 | 3.006 |
| $(CdSe)_6(PMe_3)_6$ | 2.691 | 2.709 | 1.13 | 0.62 | −0.99 | −3.37 | 3.114 |
| $(CdSe)_{10}$ | 2.649 | – | – | – | – | | 2.291 |
| $(CdSe)_{10}(PMe_3)$ | 2.762 | 2.640 | 0.24 | 0.88 | −0.40 | −0.81 | 2.369 |
| $(CdSe)_{10}(PMe_3)_2$ | 2.767 | 2.640 | 0.47 | 0.86 | −0.77 | −1.61 | 2.483 |
| $(CdSe)_{10}(PMe_3)_3$ | 2.771 | 2.653 | 0.68 | 0.80 | −0.88 | −2.25 | 2.547 |
| $(CdSe)_{10}(PMe_3)_4$ | 2.773 | 2.661 | 0.88 | 0.77 | −1.09 | −2.88 | 2.611 |
| $(CdSe)_{10}(PMe_3)_5$ | 2.772 | 2.679 | 1.05 | 0.71 | −1.13 | −3.29 | 2.654 |
| $(CdSe)_{10}(PMe_3)_6$ | 2.773 | 2.691 | 1.21 | 0.67 | −1.07 | −3.69 | 2.728 |
| $(CdSe)_{10}(PMe_3)_7$ | 2.766 | 2.711 | 1.35 | 0.62 | −1.04 | −3.90 | 2.774 |
| $(CdSe)_{10}(PMe_3)_8$ | 2.764 | 2.730 | 1.47 | 0.57 | −0.78 | −4.13 | 2.830 |
| $(CdSe)_{10}(PMe_3)_9$ | 2.780 | 2.742 | 1.59 | 0.54 | −0.69 | −4.38 | 2.893 |
| $(CdSe)_{10}(PMe_3)_{10}$ | 2.798 | 2.754 | 1.71 | 0.51 | −0.51 | −4.61 | 2.989 |

with three $PMe_3$, the P−Cd bonds of n = 10 are shorter than n = 6 and 3 by 0.010 Å and 0.124 Å, respectively. The CdSe-$PMe_3$ cluster structures are similar to those with $PH_3$ attachment (See Table S6), and have slightly shorter P–Cd bond lengths and slightly longer Se–Cd distances.

## Binding Energies

Figure 2 and S4, Table 1, S4 and S5 display the binding energy (*BE*) of the ligands capped clusters, which is defined as

$$BE = [mE^L + E^{(CdSe)n} - E^{(CdSe)nLm}]/m$$

where $E^L$, $E^{(CdSe)n}$ and $E^{(CdSe)nLm}$ are the energies of ligand, bare $(CdSe)_n$ and $(CdSe)_nL_m$ clusters, respectively. First, the attachment of ligands stabilizes the CdSe clusters. The introduction of first $PMe_3$ lowers the total energy by 0.74, 0.85, and

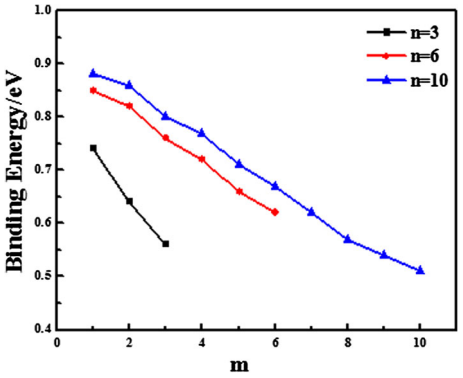


**Fig. 2** Binding energy (*BE*) of the $(CdSe)_n(PMe_3)_m$ clusters ($n = 3$, 6 and 10; m = 1–n) calculated with TPSS

0.88 eV, respectively. Second, although the *BE* decreases with increasing number of ligands, the total energy decreases further. For n = 3, 6 and 10, the *BE* decreases linearly, which indicate that the steric hindrance is significant for the small clusters. Third, the *BE* of n = 3 is lower than those of n = 6 and 10. This is unusual for small clusters with unsaturated surface atoms. From the structures in Fig. 1, one can note that the cyclic structure of n = 3 is the building block for all the large clusters. It has been characterized as a magic-sized stable structure for CdSe clusters [9, 18]. Fourth, the *BE* of CdSe-$PMe_3$ clusters is greater than that of corresponding CdSe-$PH_3$ clusters, indicating that the electron-donating group favors the binding between P-containing ligand and the CdSe clusters.

The computed enthalpies (ΔH) and Gibbs free energies (ΔG) of the ligated clusters are listed in Fig. 3, Table 1 and S6. With increasing ligand number, the ΔH of CdSe-$PMe_3$ first decreases and then increases (See Fig. 3). It is apparent that the stabilization effect is dominant at small ligand coverage, but the steric effect becomes dominant at large ligand coverage. ΔG values are positive for CdSe-$PH_3$

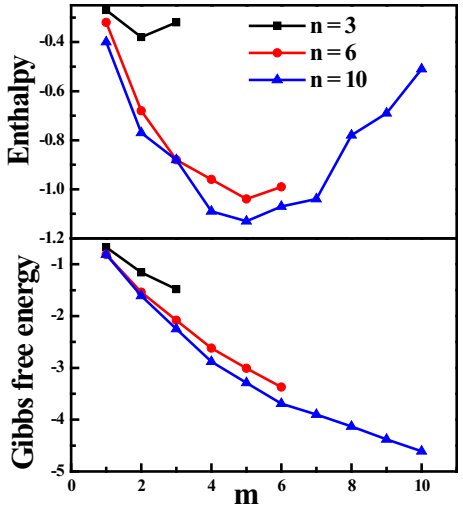


**Fig. 3** Enthalpy (ΔH, in eV) and Gibbs free energy (ΔG, in eV) of the $(CdSe)_n(PMe_3)_m$ clusters (n = 3, 6 and 10; m = 1–n) calculated with TPSS

clusters (See Table S6), and negative for CdSe-$PMe_3$ (See Table 1), indicating that CdSe-$PH_3$ is thermodynamically unstable under the computational conditions (298 K), which mainly stems from the entropy decrease of ligand attachment. Methyl groups, however, enhances the ligand–cluster interaction and makes the CdSe-$PMe_3$ clusters thermodynamically stable. For n = 3, 6 and 10, the $\Delta G$ values are negative and decrease linearly with increasing the ligands, which indicate that the $PMe_3$ ligand can cover the $(CdSe)_n$ surface and form the stable complexes. Our calculations prove that the experimentally used P-containing ligands, which have long aliphatic chains or benzene derivatives, may form thermodynamically stable structures with the CdSe nanocrystals.

## Charge Analysis

The interaction between the ligands and the clusters is also reflected by the charge-transfer features between them. The net charges on the ligands in the $PMe_3$-capped $(CdSe)_n$ clusters are shown in Table 1. In general, NBO analysis produces positive charge on the ligands, implying that electrons flow from the ligands to the clusters. There are two lone-pair 3*p* electrons on P that coordinate with the empty 5*s* orbital of Cd. As a result, the ligand serves as an electron donor and the CdSe cluster as an electron acceptor. The amount of transferred charge increases with the number of coordinated ligands, while the successive ligand donates further some charge to the cluster. For $(CdSe)_3$, the total net charge on the ligands increases from 0.22 e of m = 1 to 0.53 e of m = 3. For $(CdSe)_{10}$, the total net charge on the ligands becomes 0.24 e of m = 1 to 1.71 e of m = 10. We also found the net charge varies significantly for m = 1–5, but increase slowly for large m. The net charge on the ligands is in the range of 1.21–1.71 e for $(CdSe)_{10}(PMe_3)_m$ (m = 6–10). For the clusters with same number of ligands, the cluster with larger size has greater amount of transferred charge. For example, the transferred charge on the ligands is 0.53, 0.65 and 0.68 e for $(CdSe)_n(PMe_3)_3$ (n = 3, 6 and 10), respectively. Clusters with larger size are capable of accepting greater amount of charge. In addition, the variations in transferred charge comply with the variations in P–Cd bondlength. A short P–Cd bond favors the charge transfer between them. The amount of net charge on the ligands in the $PH_3$-capped $(CdSe)_n$ clusters are listed in Table S6. $PMe_3$ is a stronger electron donor than $PH_3$, leading to greater amount of transferred charge. For example, the transferred charge in $(CdSe)_3PMe_3$ is 0.07 e greater than that in $(CdSe)_3PH_3$.

## Optical Properties

Figures 4, 5 and 6 compare the TDDFT computed electronic absorption spectra of bare $(CdSe)_n$ and $PMe_3$-capped $(CdSe)_n$. The electronic absorption spectra of the bare clusters are basically in agreement with other computational studies [8, 16, 24]. For the bare clusters, their optical absorption is size-dependent. The band distributions are different for the bare clusters for n = 3, 6, 10. When one ligand is attached the band distribution changes accordingly. Specifically, the wavelengths of bands blue-shift and their relative locations change remarkably. For example, a

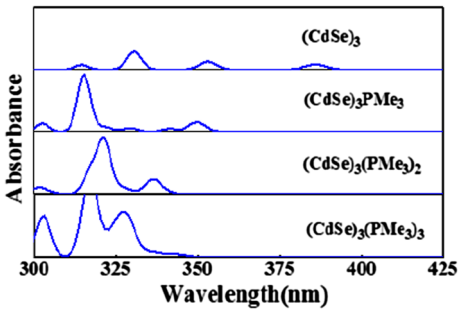


**Fig. 4** The optical absorption spectra of $(CdSe)_3$ and $(CdSe)_3(PMe_3)_m$ (m = 1–3). The *vertical axis* represents normalized absorbance ($\times 10^{-3}$) at a half-width of 3000 nm

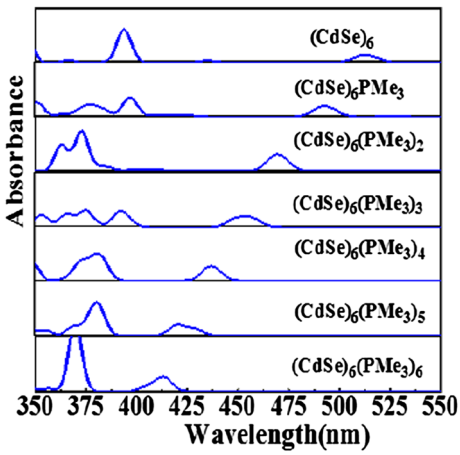


**Fig. 5** The optical absorption spectra of $(CdSe)_6$ and $(CdSe)_6(PMe_3)_m$(m = 1–6). The *vertical axis* represents normalized absorbance ($\times 10^{-3}$) at a half-width of 3000 nm

blueshift of 19 nm was noted in $(CdSe)_6PMe_3$ in comparison with $(CdSe)_6$. When the number of ligand increases, the bands blueshift further. For $(CdSe)_{10}(PMe_3)_m$, the first band changes from 505 nm at m = 1 to 422 nm at m = 10. The first bands of the clusters are mostly owing to that the transitions of the highest occupied molecular orbital (HOMO) and the lowest unoccupied molecular orbital (LUMO) as revealed by the TDDFT calculations. The first band locations of the clusters comply well with their HOMO–LUMO gaps. The gap becomes wide with increasing ligand coverage, as presented in Table 1. A wide gap usually corresponds to a short wavelength band. The size dependence of the absorption spectra can be hardly summarized from those of three sizes. A size-dependent redshift in adsorption spectra was noted from n = 3, 6 to 10 for both the bare and ligated clusters. For the bare clusters, their first bands are at 403, 512 and 540 nm, while their one ligand ligated clusters have first bands at 360, 493 and 505 nm, respectively. A similar trend was found in the clusters with two or three ligands. The TDDFT computed electronic absorption spectra of bare $(CdSe)_n$ and $PH_3$-capped $(CdSe)_n$ are shown in Figure S5-S7. The change of bands wavelengths of $PMe_3$-capped clusters is similar to that of $PH_3$-capped clusters.

The HOMO and LUMO of $(CdSe)_n$ and $(CdSe)_nPMe_3$ are depicted in Fig. 7, while those of other clusters studied in this work are given in Supplementary

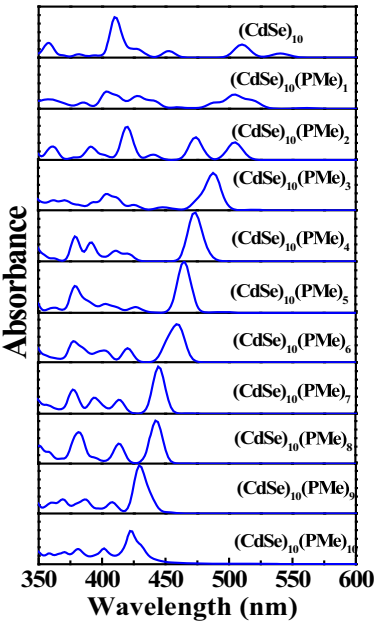


**Fig. 6** The optical absorption spectra of $(CdSe)_{10}$ and $(CdSe)_{10}(PMe_3)_m$ (m = 1–10). The *vertical axis* represents normalized absorbance ($\times 10^{-3}$) at a half-width of 3000 nm

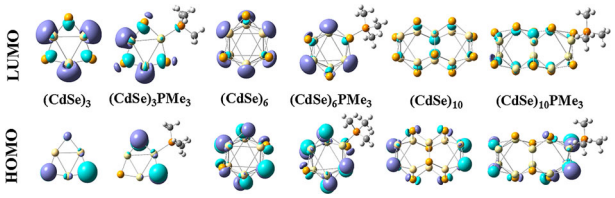


**Fig. 7** HOMO and LUMO orbitals of $(CdSe)_n$ and $(CdSe)_nPMe_3$ complexes (n = 3, 6 and 10)

material (Figures S8-S11). For the bare clusters, their HOMOs are mainly composed by the 4*p* orbitals of Se atoms, while their LUMOs by the 5*s* of Cd atoms. When ligands are attached, the HOMOs and LUMOs have similar compositions with those of corresponding bare clusters. Therefore, the attachment of ligands does not change the nature of HOMO to LUMO transitions. The electrons move from ligands to Cd atoms when the clusters are ligated, making the HOMO–LUMO transition from Se-4*p* to Cd-5*s* more difficult. As a result, the ligands lead to a blueshift trend for the clusters.

## Conclusions

The P-containing agents are often used in the preparation of CdSe nanocrystals. The structures, energetics and properties of $(CdSe)_n$ clusters (n = 3, 6 and 10) coated with $PH_3$ and $PMe_3$ ligands were studied by using density functional theory calculations with the TPSS functional and def2-TZVP basis set. The P atom in the

ligand always interacts with Cd atom. The ligand–cluster interaction was analyzed in terms of P–Cd bondlength, amount of transferred charge and interaction energy. The Se−Cd and P−Cd bond lengths increase gradually with the ligand coverage. $PMe_3$ has stronger stabilization effect on the clusters than $PH_3$. The increasing number of ligands tends to stabilize the clusters at low coverage, but the interaction energy tends to decrease at high coverage, resulting from the steric hindrance in the limited space around the cluster. The $PMe_3$ capped CdSe clusters are thermodynamically stable, as indicated by their negative Gibbs free energy under a full ligand coverage. The ligand always acts as an electron donor. The net charge transferred from the ligand to $(CdSe)_n$ increase with ligand number and cluster size. The HOMO–LUMO gaps become wide upon the ligand attachment. Accordingly, the absorption bands blueshift when the ligand is attached one by one. This is attributed to the electron-donating nature of the ligand. The incoming electrons in $(CdSe)_n$ disfavor electron transition from Se to Cd. Our study reveals the interaction between the ligands and the CdSe clusters and its influence on the structure and electronic properties of ligated clusters, providing useful information for the design and preparation of CdSe nanocrystals in presence of P-containing agents.

**Acknowledgments** Z.Z. thanks the Project of Postgraduate Degree Construction, Southwest University for Nationalities (No. 2015XWD-S0703). M.Y. thanks the financial support from National Natural Science Foundation of China (No. 21373140). S.Y. thanks the China Scholarship Council Foundation (No. 201600850004) and the Post Doctor Foundation of Institute of Atomic and Molecular Physics (No. 0020227602003).

## References

1. D. Bimberg and U. W. Pohl (2011). *Mater. Today.* **14**, 388.
2. M. Wu, P. Mukherjee, D. N. Lamont and D. H. Waldeck (2010). *J. Phys. Chem. C.* **114**, 5751.
3. Y. S. Park, A. Dmytruk, I. Dmitruk, A. Kasuya, M. Takeda, N. Ohuchi, Y. Okamoto, N. Kaji, M. Tokeshi and Y. Baba (2010). *ACS Nano.* **4**, 121.
4. C. L. Wang, S. H. Xu, L. H. Ye, L. Wei and Y. P. Cui (2011). *J. Clust. Sci.* **22**, 49.
5. X. Ji, D. Copenhaver, C. Sichmeller and X. Peng (2008). *J. Am. Chem. Soc.* **130**, 5726.
6. T. Z. Markus, S. Itzhakov, Y. I. Alkotzer, D. Cahen, G. Hodes, D. Oron and R. Naaman (2011). *J. Phys. Chem. C.* **115**, 13236.
7. R. Leitsmann and F. Bechstedt, *ACS Nano*. 11 (2009) 3505.
8. C. B. Murray, D. J. Norris and M. G. Bawendi (1993). *J. Am. Chem. Soc.* **115**, 8706.
9. E. Sanville, A. Burnin and J. J. BelBruno (2006). *J. Phys. Chem. A.* **110**, 2378.
10. C. Liu, S. Y. Chung, S. Lee, S. Weiss, and D. Neuhauser (2009). *J. Chem. Phys.* **131**, 174705.
11. P. Karamanis, G. Maroulis and C. Pouchan (2006). *J. Chem. Phys.* **124**, 071101-1.
12. R. Jose, N. U. Zhanpeisov, H. Fukumura, Y. Baba and M. Ishikawa (2006). *J. Am. Chem. Soc.* **128**, 629.
13. A. Puzder, A. J. Williamson, F. Gygi and G. Galli (2004). *Phys. Rev. Lett.* **92**, 217401-1.
14. K. A. Nguyen, P. N. Day and R. Pachter (2010). *J. Phys. Chem. C.* **114**, 16197.
15. S.V. Kilina, D.S. Kilin and O.V. Prezhdo (2009). *ACS Nano.* **3**, 93.
16. T. M. Inerbaev, A. E. Masunov, S. I. Khondaker, A. Dobrinescu, A. V. Plamadă and Y. Kawazoe (2009). *J. Chem. Phys.* **131**, 044106-1.
17. C. M. Isborn, S. V. Kilina, X. Li and O. V. Prezhdo (2008). *J. Phys. Chem. C*. **112**, 18291.
18. P. Yang, S. Tretiak and S. Ivanov (2011). *J. Clust. Sci.* **22**, 405.
19. P. Yang, S. Tretiak, A. E. Masunov and S. Ivanov (2008). *J. Chem. Phys.* **129**, 074709-1.
20. T. P. A. Ruberu, H. R. Albright, B. Callis, B. Ward, J. Cisneros, H. J. Fan and J. Vela (2012). *ACS Nano*. **6**, 5348.
21. V. V. Albert, S. A. Ivanov, S. Tretiak and S. V. Kilina (2011). *J. Phys. Chem. C.* **115**, 15793.

22. Y. Gao, B. Zhou, S. Kang, M. Xin, P. Yang, X. Dai, Z. Wang and R. Zhou (2014). *RSC Adv.* **4**, 27146.
23. S. Y. Chung, S. Lee, C. Liu and D. Neuhauser (2009). *J. Phys. Chem. B.* **113**, 292.
24. Y. Q. Cui, Z. Y. Lou, X. Q. Wang, S. P. Yu and M. L. Yang (2015). *Phys. Chem. Chem. Phys.* **17**, 9222.
25. E. Lim, A. E. Kuznetsov and D. N. Beratan (2012). *Chem. Phys.* **407**, 97.
26. A. E. Kuznetsov, D. Balamurugan, S. S. Skourtis and D. N. Beratan (2012). *J. Phys. Chem. C.* **116**, 6817.
27. C. J. Murphy (1996). *J. Clust. Sci.* **7**, 341.
28. X. Q. Wang, Q. Zeng, J. Shi, G. Jiang, M. L. Yang, X. Y. Liu, G. Enright and K. Yu (2013). *Chem. Phys. Lett.* **568**, 125.
29. J. M. Azpiroz, J. M. Matxain, I. Infante, X. Lopez and J. M. Ugalde (2013). *Phys. Chem. Chem. Phys.* **15**, 10996.
30. M. D. Ben, R. W. A. Havenith, R. Broer and M. Stener (2011). *J. Phys. Chem. C.* **115**, 16782.
31. J. Tao, J. P. Perdew, V. N. Staroverov and G. E. Scuseria (2003). *Phys. Rev. Lett.* **91**, 146401-1.
32. D. Andrae, U. Haeussermann, M. Dolg, H. Stoll and H. Preuss (1990). *Theor Chim Acta.* **77**, 123.
33. TURBOMOLE V5-9-1. University of Karlsruhe (2007).
34. J. P. Perdew, K. Burke and M. Ernzerhof (1996). *Phys. Rev. Lett.* **77**, 3865.
35. A. D. Becke (1988). *Phys. Rev. A.* **38**, 3098.
36. C. L. Lee, W. Yang and R. G. Parr (1988). *Phys. Rev. B.* **37**, 785.
37. J. H. Wood and A. M. Boring (1978). *Phys. Rev. B.* **18**, 2701.
38. K. Eichkorn, O. Treutler, H. Oehm, M. Haeser and R. Ahlrichs (1995). *Chem. Phys. Lett.* **242**, 652.
39. M. Sierka, A. Hogekamp and R. Ahlrichs (2003). *J. Chem. Phys.* **118**, 9136.
40. M. E. Casida, in D. P. Chong (ed.), *Recent Advances in Density Functional Methods* (World Scientific Publishing Co Pvt. Ltd., Singapore, 1995).
41. E. D. Glendening, J. K. Badenhoop, A. E. Reed, J. E. Carpenter, J. A. Bohmann, C. M. Morales, C. R. Landis and F. Weinhold, NBO6.0, Theoretical Chemistry Institute, University of Wisconsin, Madison (2013).
42. W. R. Wadt and P. J. Hay (1985). *J. Chem. Phys.* **82**, 284.
43. P. J. Hay and W. R. Wadt (1985). *J. Chem. Phys.* **82**, 270.
44. M. J. Frisch, G. W. Trucks, H. B. Schlegel, G. E. Scuseria, M. A. Robb, J. R. Cheeseman, G. Scalmani, V. Barone, B. Mennucci, G. A. Petersson, H. Nakatsuji, M. Caricato, X. Li, H. P. Hratchian, A. F. Izmaylov, J. Bloino, G. Zheng, J. L. Sonnenberg, M. Hada, M. Ehara, K. Toyota, R. Fukuda, J. Hasegawa, M. Ishida, T. Nakajima,Y. Honda, O. Kitao, H. Nakai, T. Vreven, J. J. A. Montgomery, J. E. Peralta, F. Ogliaro, M. Bearpark, J. J. Heyd, E. Brothers, K. N. Kudin, V. N. Staroverov, R. Kobayashi, J. Normand, K. Raghavachari, A. Rendell, J. C. Burant, S. S. Iyengar, J. Tomasi, M. Cossi, N. Rega, J. M. Millam, M. Klene, J. E. Knox, J. B. Cross, V. Bakken, C. Adamo, J. Jaramillo, R. Gomperts, R. E. Stratmann, O. Yazyev, A. J. Austin, R. Cammi, C. Pomelli, J. W. Ochterski, R. L. Martin, K. Morokuma, V. G. Zakrzewski, G. A. Voth, P. Salvador, J. J. Dannenberg, S. Dapprich, A. D. Daniels, O. Farkas, J. B. Foresman, J. V. Ortiz, J. Cioslowski and D. J. Fox *GAUSSIAN09, Revision A.01, Gaussian, Inc*. (Wallingford, CT, 2009).